Available online at www.sciencedirect.com
ScienceDirect
Journal of the European Ceramic Society 31 (2011) 2057–2063
www.elsevier.com/locate/jeurceramsoc

Granite as flux in stoneware tile manufacturing

H.F. El-Maghraby [a], Mohamed M. El-Omla [b], F. Bondioli [c], S.M. Naga [a,*]

[a] Department of Ceramics, National Research Centre, Cairo, Egypt
[b] Department of Geology, Suez Canal University, Ismailia, Egypt
[c] Department of Materials and Environmental Engineering, Faculty of Engineering University of Modena and Reggio Emilia, Modena, Italy

Received 2 February 2011; received in revised form 4 May 2011; accepted 16 May 2011
Available online 8 June 2011

Abstract

Natural granite was used to completely replace both feldspathic and inert components of a traditional ceramic body. Raw material from Sinai (Egypt) was added (in the range 20–35 wt%) to a commercial Egyptian ball clays (from Aswan, Egypt) in order to obtain laboratory tiles sintered at 1220 °C.

Densification was studied according to ISO rules, while sinterability was estimated by optical dilatometry. Chemical, physical and microstructural analyses were accomplished to find the relationship between both the phase composition and microstructure of the fired bodies properties. The fired samples show moderate thermal expansion as well as reasonable bending strength. Therefore, as a nonconventional raw material in the modern ceramic production, the studied batches are recommended for the production of industrial fast firing tiles showing properties similar to commercial ceramic floor and/or wall tiles.

Keywords: Granite; Stoneware; Microstructure; Dilatometric behavior

1. Introduction

Over the last decades, the ceramic tile industry has progressively shifted its production toward new materials with excellent technical properties that are able to successfully compete with ornamental stones.[1,2] These products are manufactured using clay, quartz and large amounts of fluxes such as sodic and potassic feldspars.[3] However the high price of feldspar has a remarkable impact on the cost of the end-product. Therefore, many of the recent studies related to stoneware compositions concerned the substitution of the traditional fluxes with other low cost minerals and/or waste.[4] Some promising results were obtained using glass cullet,[5,6] cathode ray tube (CRT) glass,[7,8] different industrial wastes[9,10] as well as some volcanic ash and zeolite rich rocks.[11,12] Other igneous rocks such as, nepheline synite,[13–15] gabbro,[16] granite,[17–19] basalt[20,21] and basaltic tuffs[22,23] were successfully used to produce vitrified ceramic tiles on firing at temperature ranging between 900 and 1300 °C.

The aim of this study was to evaluate the possibility to use natural granite in the manufacture of ceramic products. Different compositions using only ball clays, Kalabsha clay from Aswan area (Egypt), and natural granite from Sinai (Egypt) were tailored to completely replace both feldspatic and inert components of a traditional ceramic body.

Granite is an intrusive holocrystalline rock characterized by medium and fine grain structure which usually consists of orthoclase, acidic plagioclase, and quartz. Magnesia and ferruginous compounds (hornblends, biotite, muscovite, and others) can also be present in granites as accessory minerals. Another characteristic feature of pegmatites, which is due to their semideep bedding in the Earth's crust, is the so-called pigmatoid structure characterized by coarse grains (sometimes even gigantic grains of industrial mineral components) and regular intergrowth of quartz and feldspars.[24]

In this study the exclusive use of Egyptian raw materials was tested in order to verify the possibility to use only local raw materials to obtain ceramic materials with high added value instead of proceed to import them also for the local production. In fact even if in the ceramic field the technology is widely well-known, further research is mandatory to reduce the general environmental impact. The possibility and the importance for

* Corresponding author. Tel.: +20 122174737; fax: +20 233370931.
E-mail addresses: salmanaga@yahoo.com, ss.naga@nrc.sci.eg (S.M. Naga).

0955-2219/$ – see front matter © 2011 Elsevier Ltd. All rights reserved.
doi:10.1016/j.jeurceramsoc.2011.05.023

Table 1
Chemical analysis of the used raw materials (oxide wt%).

Constituents	Kalabsha clay	Granite
SiO_2	47.35	75.86
Al_2O_3	36.12	11.45
Fe_2O_3	0.77	2.48
TiO_2	2.22	0.24
CaO	0.77	0.31
MnO	0.00	0.05
MgO	0.10	0.26
Na_2O	0.11	3.35
K_2O	0.14	5.95
P_2O_5	0.00	0.03
L.O.I.	12.42	0.02
Total	100.00	100.00

the ceramic industry to obtain less expensive materials from an energetic point of view is securely very high also because it is reflected on the total production costs. Moreover, in this work the use of granite could help to achieve the complete bodies densification at low firing temperature. In fact during firing both the feldspar and mica present in granite could favor the formation of a liquid phase that could contribute to obtain the final ceramic products at lower temperature.

In particular the interest was focused on the effect of granite content (20–35 wt%) on the properties of the obtained laboratory tiles that were characterized in accordance of ISO rules in order to define their UNI EN ISO classification.

2. Experimental

2.1. Raw materials

Egyptian raw materials, Kalabsha clay from Aswan and granite from Sinai, were selected and characterized for the present study. Chemical and mineralogical compositions are reported in Tables 1 and 2, respectively.

2.2. Processing

The raw materials were ground separately to pass 200 mesh (0.75 mm) sieve. Four mixtures were prepared by adding 20, 25, 30, and 35 wt% of granite to the clay (sample codes S1, S2, S3 and S4). The batch compositions are reported in Table 3.

Table 2
Mineralogical composition of raw materials.

Rational constituents (wt%)	Kalabsha clay	Granite
Albite	0.9	37.06
Orthoclase	0.8	30.67
Anorthite	3.8	3.42
Kaolinite	86.8	–
Free quartz	4.1	22.25
Diposide	–	3.26
Pyroxene	–	1.39
Apatite	–	0.28
Ilmenite	–	0.80
Magnetite	–	0.94

Table 3
Batch composition of the prepared mixture and their fluxing oxides content.

Batch	Granite (wt%)	Clay (wt%)
S1	20	80
S2	25	75
S3	30	70
S4	35	65

The obtained mixtures were experimented at a laboratory scale, simulating the industrial tilemaking process: batches (100 g each) were prepared by dry milling for 30 min in a laboratory ball mill using alumina grinding media, followed by sieving below 63 μm. The dried powders were humidified to a water content of 6 wt% and uniaxially pressed at 40 MPa to produce rectangular tiles ($11 \times 5.5 \times 8\ mm^3$). The green compacts were dried at 105 °C up to constant weight before firing, then fired in an industrial kiln at 1220 °C with a firing cycle of 50 min.

2.3. Characterization

The dilatometric behavior of the green mixtures was determined using a vertical optical non-contact dilatometer with 15 mm sample height (model Misura, Expert System Solution, I). For this measurement, the pressed samples of $15 \times 4 \times 4\ mm^3$ were heated from 20 to 1400 °C with heating rate of 50 °C/min.

The thermal behavior of the starting materials was investigated by DTA (Netzch STA 409), at a heating rate of 10 °C/min up to 1000 °C.

The densification obtained after the sintering step was described in terms of water absorption, as required by UNI EN ISO 10545.3, together with linear shrinkage, bulk density and apparent porosity according to the ASTM C20-74. The coefficient of reversible linear thermal expansion was determined using a horizontal dilatometer (NETZSCH, 402 EP) with a heating rate of 10 °C/min up to 1000 °C.

The bending strength of the fired samples was measured using a three-point loading method with a spam of 80 mm (Flexometer, CCR, Faenza, Italy) according to the UNI EN ISO 10545.4.

X-ray diffraction (XRD) measurements were carried out on the powdered sintered samples in order to qualitatively evaluate the crystalline phases, using a powder diffractometer (PW 3710, Philips Research Laboratories, Netherlands) with Ni-filtered CuKα radiation. The peaks area of mullite (at $d = 5.39$ Å, $I = 50$), cristobalite (at $d = 4.05$ Å, $I = 100$) and quartz (at $d = 4.26$ Å, $I = 35$) was determined in order to compare their content in the different studied batches. The peak area is calculated by multiplying the width at half of the selected peak by its height.

The microstructure of the fired bodies was examined by scanning electron microscopy (SEM, Model XL30, Philips Research Laboratories) coupled with an energy dispersion spectroscopy (EDS, INCA 350, OXFORD) equipment, both on etched and non-etched fractured surfaces of the bodies.

Colorimetric measures were performed by UV-Vis spectrophotometer (Perkin Elmer, Lambda 19) using CIE Lab color space (Illuminant D65, observer 10°). The L^*, a^*, and b^* parameters were calculated by the Hunter method.[25]

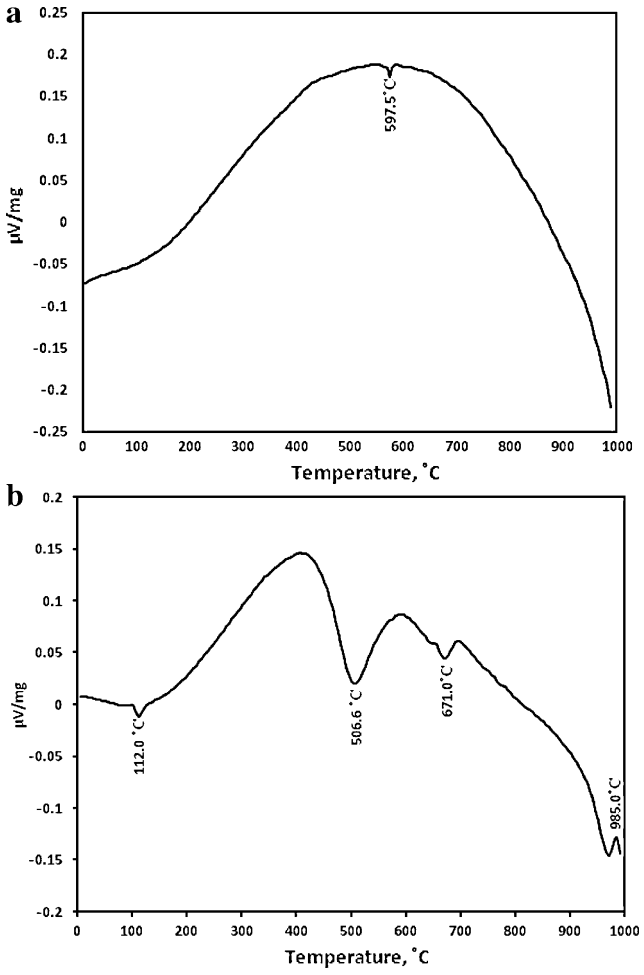

Fig. 1. DTA curves of granite (a) and Kalabsha clay (b).

3. Results and discussion

The chemical and mineralogical compositions of the used raw materials are reported in Tables 1 and 2, respectively. Kalabsha clay consists mostly of kaolinite, quartz, and anorthite, while granite is composed of quartz and feldspatic minerals such as orthoclase, albite, and anorthite together with diopside. The chemical analysis is coherent with the diffractometric results underlining that the chromophore oxides, in particular Fe_2O_3 and TiO_2, that can influence the color developed in a ceramic matrix, are quite abundant.

The DTA curve of the granite sample (Fig. 1a) shows low intensity endothermic peak at 597.5 °C indicating the polymorphic transformation of low → high quartz, which is a major mineral in the granite. Fig. 1b shows the DTA curve recorded for Kalabsha clay characterized by the presence of four endothermic peaks. First endothermic peak, at around 112 °C, was related to the removal of adsorbed water. The next endothermic peaks are related to the characteristic thermal behavior of kaolinite, the main mineralogical constituent of the used clay. In particular the peak at 506 °C is mainly attributed to the dehydroxylation of the clay mineral (kaolinite), the peak at 671 °C to the formation of metakaolinite whereas the last endothermic peak at 985 °C could be attributed to structural reorganization and formation of new crystalline phases, e.g. silica-rich γ-Al_2O_3 having the spinel structure.

The sinterability of the green mixtures obtained by milling granite with the commercial clay was defined by an optical non-contact dilatometer. The obtained curves allowed to estimate the initial sintering temperature and the temperature of maximum sintering rate. In Fig. 2 the dilatometric curves of the samples containing 20 (S1), 25 (S2), 30 (S3) and 35 wt% (S4) of gran-

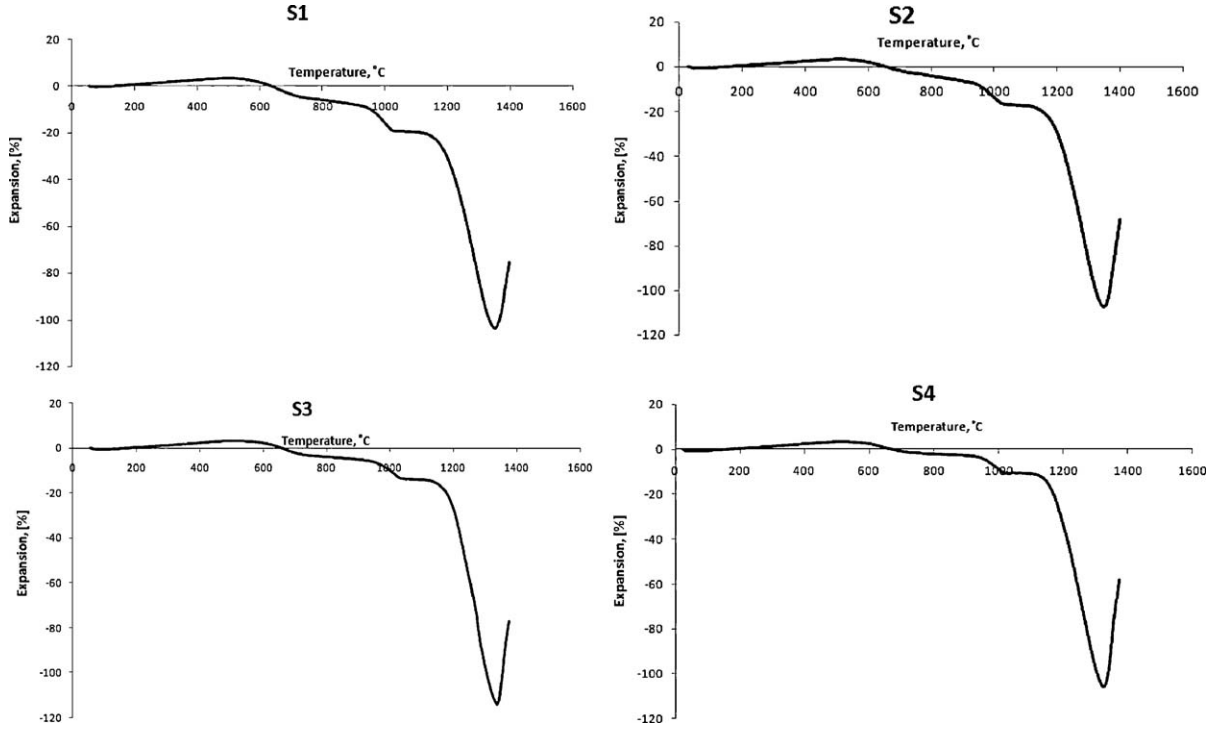

Fig. 2. Dilatometric curves of the samples containing 20 (S1) and 35 (S4) wt% of granite.

ite are plotted as representative. Independently from the granite content, the samples initially present a thermal expansion until ≈550 °C and successively, after two decomposition steps, start to sinter at ≈1150 °C. In particular the sharp shrinkage behavior in the range 98–1000 °C was attributed to a transformation reaction in which SiO_4 groups combine with the AlO_6 groups to form the Al–Si spinel phase. The increase of granite content of the bodies led to the presence of additional fluxing ions, which activates this transformation and produces a decreasing of the transformation temperature.

Regarding the temperature of maximum sintering rate, identified by the negative peak on the first derivate curve, decreases (from 1281 for 20 wt% to 1253 °C for 35 wt%) as the granite content is increased. This behavior is due to the low viscosity of glassy phase which favors the enhancement of sintering kinetics. These results evidence the fluxing nature of this natural material and it can be noticed that the shrinkage of the mixtures increases in an exponential form with temperature.

The mineralogical behavior of the fired samples at the studied temperature (1220 °C) as a function of granite content (Fig. 3) pointed out that the whole samples present quartz [ICDD (01-085-0794)] and mullite [ICDD (01-089-2814)] as main crystalline phase and, as minor phase, cristobalite [ICDD (01-082-0512)], albite [ICDD (00-001-0739)], and anorthite [ICDD (01-076-0948)]. In particular mullite and cristobalite contents decrease as the granite content is increased (Fig. 4). Regarding the inert phase, with the only exception of S4 composition, the quartz content, as expected, increases as the granite is increased. This is probably due to the formation, at the higher granite content, of an aggressive glassy phase rich in iron, alkaline, and earth alkaline ions that activates the quartz dissolution and decreases residual quartz content.

Sintering degree was studied in terms of linear shrinkage (LS%), water absorption (WA%) and apparent density measured as a function of granite content on the tiles sintered at 1220 °C (Table 4).

The water absorption, strictly related to the material microstructure and to the open porosity, significantly decreases as the granite content is increased. Moreover the apparent density values and LS% indicate an enhancement of the densification process as the granite content is increased with an important decrease of the apparent porosity. It is possible to conclude that the increase in granite content increases the bodies content of the liquid phase. During vitrification, the formed liquid phase migrates through the open pore microstructure and fills it.

According to the UNI EN ISO standards and on the basis of water absorption percentage the obtained tile samples could

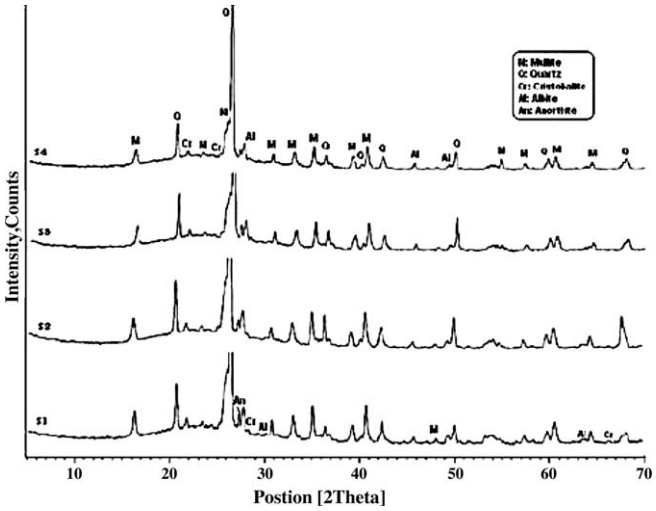

Fig. 3. X-ray diffraction patterns of fired bodies S1–S4.

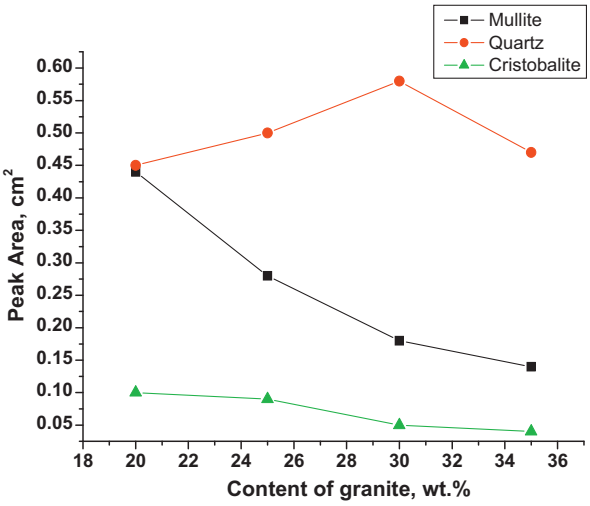

Fig. 4. XRD peak area of mullite, quartz, and cristobalite phases.

be classified into BIIa (S1, S2 and S3) and BIb (S4) groups having WA $3\% \leq E \leq 6\%$ and $0.5\% \leq E \leq 3\%$, respectively, and belong to (medium water absorption) semi-vitrified and (low water absorption) vitrified ceramic tiles.[27]

Finally, the mixes showed in general moderate thermal expansion coefficients between 20 and 1000 °C (Table 4) that increases with the increase of granite content (from 6.15×10^{-6} to 6.34×10^{-6}).

The microstructure of the S1 and S4 bodies depicts the typical features of a well-fired ceramic body in which all the physical

Table 4
Linear shrinkage (LS%), water absorption (WA%), apparent density (AD), apparent porosity (AP%), bending strength (MPa) and thermal expansion coefficient (α) of the sintered samples as a function of granite content compared with respect to a commercial product.

Sample	LS (%)	WA (%)	AD (g/cm^3)	AP (%)	BS (MPa)	α ($\times 10^{-6}$)
S1	7.90 ± 0.01	5.1 ± 0.01	2.23	11.20	–	–
S2	8.00 ± 0.01	4.03 ± 0.01	2.25	9.06	24.36	6.15
S3	8.20 ± 0.01	3.56 ± 0.01	2.27	7.15	31.20	6.29
S4	8.70 ± 0.01	2.47 ± 0.01	2.30	5.56	31.81	6.34

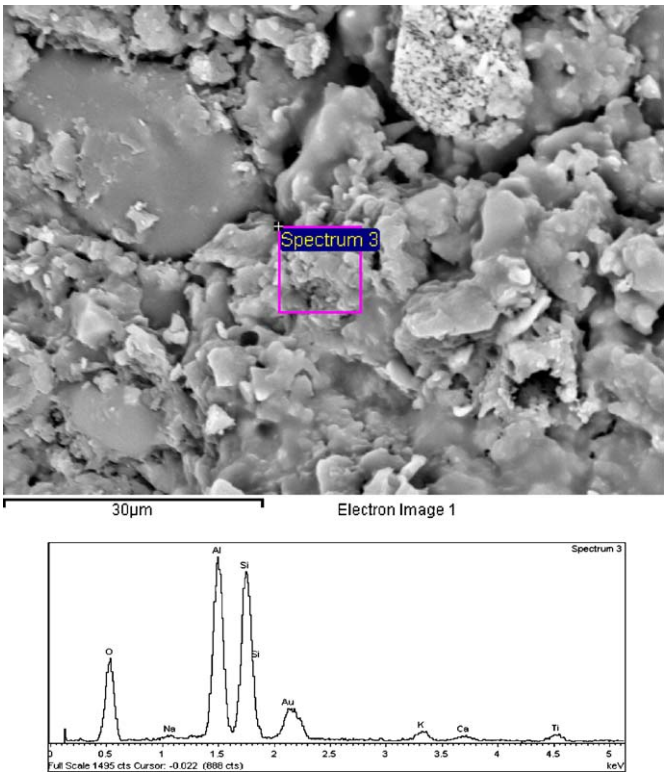

Fig. 5. SEM micrograph of non-etched fracture surface of S1 sample fired at 1220 °C and its EDS spectra.

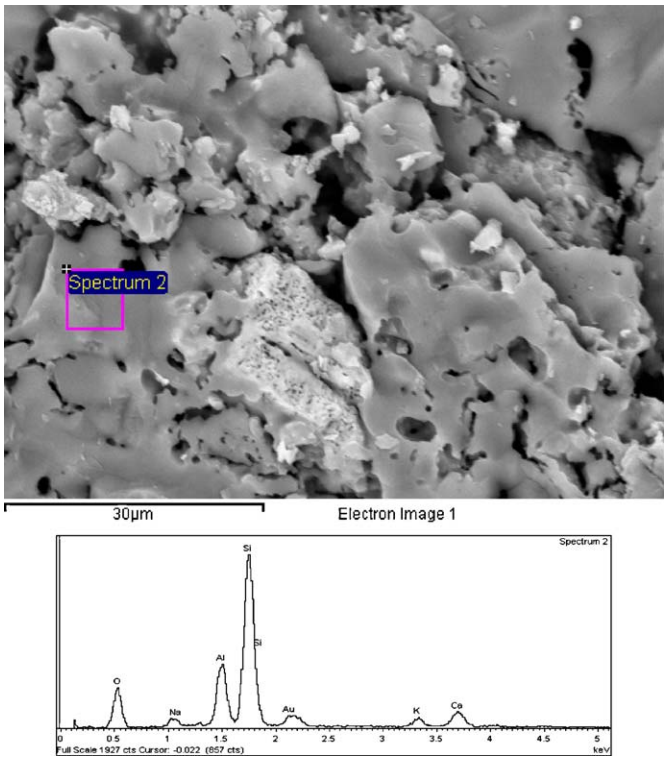

Fig. 6. SEM micrograph of non-etched fracture surface of S4 sample fired at 1220 °C and its EDS spectra.

transformations and chemical reactions between the original raw materials have taken place. The presence of areas with different morphologies is clearly observed. Such areas correspond to amorphous regions (Figs. 5 and 6). Furthermore, etched samples (Fig. 7) show etch pits which are a typical microstructural feature of etched glasses[26] and hence, those regions are likely feldspar derived glassy phase. Regions including mullite crystals with two different morphologies can be distinguished in Figs. 7 and 8. Primary mullite with fine mullite crystals derived from clay relicts show similar morphology to that found in early studies of mullite formation from thermal decomposition of pure kaolinite.[28] Moreover, needle-like mullite crystals having fine and coarse nature are also observed corresponding to secondary mullite formed from regions in which feldspar has penetrated clay agglomerates. It is noticed that primary mullite is usually adjacent to regions of secondary needle-like mullite crystals. This suggests that primary mullite crystals formed from clay could grow and transform into secondary mullite crystals if they are near to a lower viscosity matrix. This result is in agreement with Màrquez et al.[30] Moreover the SEM micrographs show that the edges of quartz particles are rounded, indicating their partial dissolution in the formed liquid phase.[30] Some of these quartz particles show micro-cracks (Fig. 9), likely due to both the α–β phase transformation of quartz crystals taking place at 573 °C and to the relaxation of micro-stresses originated between quartz grains and the surrounding glassy phase by the differences in their thermal expansion coefficients.[29]

The values of the bending strength measured on the different obtained tiles (Table 4) show that it is affected by the porosity and granite content. In fact two factors have influence on the bending strength of a fired bodies. The first is relating to the phenomenon known as the pre-stressing effect. Quartz is the most abundant crystalline phase present in the fired bodies. The difference between the thermal expansion coefficients of the quartz and the matrix has a strengthening effect, since it subjected the matrix to microscopic residual compressive stresses that originates during the cooling phase of the firing cycle. The larger these stresses are, the higher is the strength of the ceramic body.[31,32] The increase in S3 bending strength in comparison to S2 is due to this effect. The slight increase in S4 bending strength value is due to the quartz presence and the decrease of its porosity. Generally, bending strength in ceramics decreases

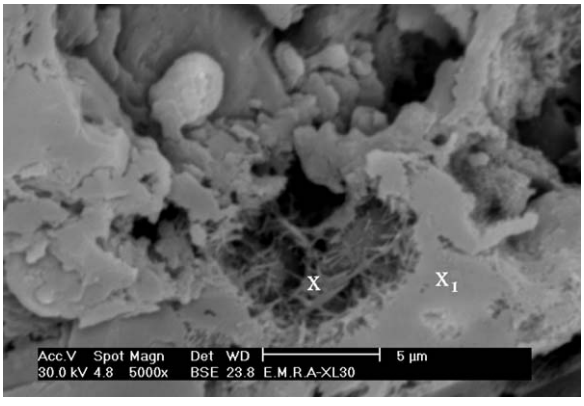

Fig. 7. SEM micrograph of etched S1 fired sample showing primary (X1) and secondary (X) mullite regions.

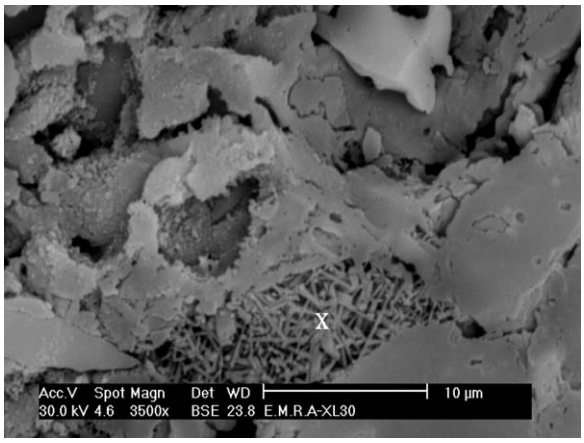

Fig. 8. SEM micrograph of etched S4 fired sample showing coarse needle-like secondary mullite (X) regions.

exponentially by increasing porosity, and the denser the fired bodies is the higher the bending strength is.[33]

The second factor is the morphology of secondary mullite needles which has a great effect on the bending strength values. The increase in S4 bending strength is related additionally to the presence of coarse needle-like secondary mullite. The liquid phase developed in S4 is rich in fluxing ions and accordingly, has a lower viscosity, in comparison with other mixes (Table 3 and Figs. 7 and 8). The lower viscosity of the liquid phase allows the crystallization of needle-like secondary mullite, having a rather aspect ratio. This is in agreement with the results reported by Màrquez et al.[30] However, the samples show values higher than those prescribed in the EN ISO 10545.4 rule for the floor tiles materials (>22 MPa for BIIa, 30 MPa for BIb).

From the colorimetric analysis, L^* and b^* values decreases as the granite content is increased while the opposite trend characterized the a^* parameter (Table 5). This behavior is due to the chemical composition of the used raw materials. In fact, as the granite content is increased, TiO_2, mainly present in the Aswan clay, decreases as the L^* and b^* values and Fe_2O_3, mainly present in granite, increases as a^* parameter. In general, however, the obtained values are compatible with white single fired floor tiles.

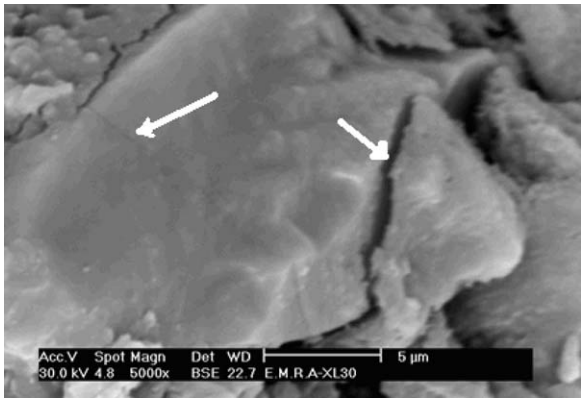

Fig. 9. SEM micrograph of etched S1 fired sample showing cracked quartz particle.

Table 5
CIE-LAB parameters of the fired bodies S1–S4.

Samples	L^*	a^*	b^*
S1	79.66	2.91	16.87
S2	76.89	2.92	15.66
S3	72.68	3.25	15.29
S4	69.26	3.38	14.77

4. Conclusions

The environmental and economical advantages obtained from this study confirm the feasibility of use of natural granite in a ceramic formulation. The result was achieved without substantially modifying the process and the technological conditions and therefore avoiding raw materials import, with relative potential pollution. The laboratory samples obtained show main properties similar to commercial ceramic products and can be classified into BIIa (S1, S2 and S3) and BIb (S4) groups having WA $3\% \leq E \leq 6\%$ and $0.5\% \leq E \leq 3\%$, respectively, corresponding to single firing tiles mainly used for floor or wall covering.

Acknowledgements

This work has been carried out within the project "Transfer of innovative technology of dry milling for high value ceramic product with low environmental impact", Italian-Egypt executive program for scientific and technological co-operation (2008–2010), MAE.

References

1. Burzacchini P. Porcelain tile, its history, and development. *Ceram World Rev* 2000;**10**(37):96–103.
2. Esposito L, Tucci A, Naldi D. The reliability of polished porcelain stoneware tiles. *J Eur Ceram Soc* 2005;**25**(9):1487–98.
3. Dondi M. Compositional parameters to evaluate feldspathic fluxes for ceramic tiles. *Tile Brick Int* 1994;**10**(2):77–84.
4. Tucci A, Esposito L, Rastelli E, Palmonari C, Rambaldi E. Use of soda-lime scrap-glass as a fluxing agent in a porcelain stoneware tile mix. *J Eur Ceram Soc* 2004;**24**:83–92.
5. Maschio S, Furlani E, Tonello G, Faraone N, Aneggi E, Minichelli D, Fedrizzi L, Bachiorrini A, Bruckner S. Fast firing of tiles containing paper mill sludge, glass cullet, and clay. *Waste Manag* 2009;**29**(11): 2880–5.
6. Rambaldi R. Recycled glass tiles. *Ceram World Rev* 1999;**9**(33):234–9.
7. Andreola F, Barbieri L, Karamanova E, Lancellotti I, Pelino M. Recycling of CRT panel glass as fluxing agent in the porcelain stoneware tile production. *Ceram Int* 2008;**34**(5):1289–95.
8. Andreola F, Barbieri L, Bondioli F, Ferrari AM, Miselli P. Recycling of screen glass into new traditional ceramics materials. *Int J Appl Ceram Technol* 2010;**7**(6):909–17.
9. El-Maghraby A, Naga SM. Industrial wastes as raw materials for tiles making. *Sil Ind* 2003;**68**(7–8):89–92.
10. Sakolar R, Smetanova L. Dry pressed ceramic tiles based on fly ash-clay body: influence of fly ash granulometry and pentasodium triphosphate addition. *Ceram Int* 2010;**36**(1):215–21.
11. dè Gennaro R, Cappelletti P, Cerri G, dè Gennaro M, Dondi M, Guarini G, Langella A, Naimo D. Influence of zeolites on the sintering and technological properties of porcelain stoneware tiles. *J Eur Ceram Soc* 2003;**23**:2237–45.

12. dè Gennaro R, Dondi M, Cappelletti P, Cerri G, dè Gennaro M, Guarini G, Langella A, Parlato L, Zanelli C. Zeolite–feldspar epiclastic rocks as flux in ceramic tile manufacturing. *Micropor Mesopor Mater* 2007;**105**:273–8.
13. Ibrahim DM, Sallam EH, Khalil AA, Naga SM. Nepheline syenite–talc low temperature vitrified bodies. *Ceram Int* 1981;**7**:69–72.
14. Burat F, Kangal O, Onal G. An alternative mineral in the glass and ceramic industry: nepheline syenite. *Miner Eng* 2006;**19**:370–1.
15. Salem A, Jazayeri SH, Rastelli E, Timellini G. Dilatometric study of shrinkage during sintering process for porcelain stoneware body in presence of nepheline syenite. *J Mater Process Technol* 2009;**209**:1240–6.
16. Sallam EH, Naga SM, Ibrahim DM. Clay–gabbro mixtures. *Interbrick* 1987;**3**(2):13–4.
17. Ibrahim DM, Sallam EH, Naga SM. Effect of the degree of crystallinity of flux on tile bodies. *TBI* 1990;**6**(1):7–10.
18. Ryshchenko MI, Shchukina LP, Fedorenko EYu, Firsov KN. Possibility of obtaining ceramogranite using quartz–feldspar raw material from Ukraine. *Glass Ceram* 2008;**65**(1–2):23–6.
19. Tereshchenko IM, Pun' Ko GN, Serikova LV. Optimization of ceramic granite composite compositions. *Glass Ceram* 2000;**57**(11–12):435–7.
20. Sallam EH, Khalil AA, Naga SM, Ibrahim DM. China clay–basalt mixtures. *Trans J Br Ceram Soc* 1982;**81**:156–9.
21. Naga SM, Sallam EMH, Abd El-Aziz D. Assessment of some Egyptian basalt and low-grade clays for ceramic tiles manufacture. *Ind Ceram* 1993;**13**(3–4):143–8.
22. Ergul S, Akyildiz M, Karamanov A. Ceramic material from basaltic tuffs. *Ind Ceram* 2007;**27**(2):89–94.
23. Ergul S, Ferrante F, Pisciella P, Karamanov A, Pelino M. Characterization of basaltic tuffs and their applications for the production of ceramic and glass–ceramic materials. *Ceram Int* 2009;**35**:2789–95.
24. Goncharova YuI, Stokova VV. *Mineralogy and photography of raw materials production of construction and technical ceramics. I2d*. Belgorad: Be IGTASM; 2001.
25. Lewis PA. *Pigments Handbook*, vol. 1. New York: John Wiley & Sons; 1988.
26. Worrall WC. *Clays and ceramic raw materials*. London: Applied Science Publ.; 1988.
27. Single firing technical characteristics, UNI EN 14411 (ISO 13006).
28. Homer PN, Crauford BJ. The microstructure of etched glass surfaces. *Glass Technol* 1970;**11**:10–4.
29. Chen CY, Lan GS, Tuan WH. Microstructural evolution of mullite during the sintering of kaolin powder compacts. *Ceram Int* 2000;**26**: 515–720.
30. Màrquez JM, Rincòn JMa, Romero M. Mullite development on firing in porcelain stoneware bodies. *J Eur Ceram Soc* 2010;**30**:1599–607.
31. Màrquez JM, Rincòn JMa, Romero M. Effect of firing temperature on sintering of porcelain stoneware tiles. *Ceram Int* 2008;**34**:1867–73.
32. Carty WM, Senapati U. Porcelain—raw materials, processing, phase evolution, and mechanical behaviour. *J Am Ceram Soc* 1998;**81**(1):3–20.
33. Statbis G, Ekonomakou A, Stournaras CJ, Ftikas C. Effect of firing conditions, filler grain size and quartz content on bending strength and physical properties of sanitaryware porcelain. *J Eur Ceram Soc* 2004;**24**: 2357–66.